

Resin-trapped gold nanoparticles: An efficient catalyst for reduction of nitro compounds and Suzuki-Miyaura coupling



Dipen Shah, Harjinder Kaur*

Department of Chemistry, School of Sciences, Gujarat University, Ahmedabad, India

ARTICLE INFO

Article history:

Received 23 August 2013

Received in revised form 7 October 2013

Accepted 8 October 2013

Available online 17 October 2013

Keywords:

Resin impregnated AuNPs

Nitroarenes reduction

Suzuki-Miyaura reaction

Microwave heating

ABSTRACT

Gold in nanoparticle form shows good catalytic activity in contrast to bulk form and is finding applications in a variety of organic reactions. The present investigation describes direct deposition of gold nanoparticles onto commercially available resin by sorption reduction method. Uniformly dispersed nanoparticles of 3–8 nm dimensions were characterized by UV-visible spectroscopy, XRD, SEM and TEM, etc. The AuNPs were found to be remarkably stable and active catalysts for the selective reduction of nitro group under mild reaction conditions and microwave-assisted ligand-free Suzuki-Miyaura cross-coupling reaction between aryl halides and phenylboronic acid. Calculated rate constant ($2.5 \times 10^{-2} \text{ s}^{-1}$) for the reduction of 4-nitrophenol is among the best reported in the literature. The versatility of both the protocols is demonstrated by taking a number of substrates.

© 2013 Elsevier B.V. All rights reserved.

1. Introduction

Today, noble metals are being used as catalysts in the synthesis of a variety of important organic compounds. An efficient, recyclable and cost-effective synthesis of noble metal nanocatalysts is of great importance as it allows effective utilization of these expensive metals. Two key factors that determine the catalytic performance of such nanocatalysts are the particle size and the supports used for the dispersion of the noble metals [1]. Small size of the particles enhances their surface area and hence the number of reactive sites. On the other hand, choice of support plays a crucial role in the accessibility to catalytic sites. In the last few decades, gold nanoparticles (AuNPs) have been used in many areas of research including electronics, biomedicines, optics, and catalysis due to their strong optical, electrical, and chemical properties, as well as their biocompatible nature. Catalytic activity has been extensively reviewed in many reactions of both, industrial and environmental importance [2]. To facilitate catalyst recovery, AuNPs are usually dispersed onto solid matrices to prepare heterogeneous AuNP catalysts. According to the literature [3–8], various materials have been used as supporting matrices, including carbon nanotubes, silica, titania, ceria alumina, polymers, etc. Amongst them, alumina is one of the most frequently used supports owing to its remarkable properties such as high surface area, porous structure and good mechanical strength [9,10]. The impregnation method is a general strategy for the heterogenization of AuNPs [11,12]. How-

ever, the resultant catalysts often suffer from a significant loss of catalytic activity during recycling because of weak interactions between the AuNPs and supporting matrices. To overcome these disadvantages, much effort has been paid to the development of new methodologies for the heterogenization of AuNPs. Yang et al. [13] have used of an organic gel based on polymeric phloroglucinol carboxylic acid and formaldehyde to support gold nanoparticles. Li et al. [14] have synthesized stable AuNPs encapsulated in a silica dendrimer organic-inorganic hybrid support as a recyclable catalyst for the oxidation of alcohols. Ohno et al. employed high density poly (methyl methacrylate) brushes to increase dispersion of gold nanoparticles [15]. Miyamura et al. [16] have reported polystyrene supported AuNPs as a catalyst for the aerobic oxidation of alcohols to aldehydes and ketones under atmospheric conditions.

We have earlier synthesized palladium nanoparticles supported on Amberlite XAD-4 and found that the resulting catalyst was not only stable and recyclable but also showed catalytic activity comparable to colloidal nanoparticles [17,18]. This prompted us to study the catalytic behavior of other metals on this support. In the present work, we have evaluated the catalytic activity of resin-trapped AuNPs toward reduction of nitro compounds and the Suzuki-Miyaura cross-coupling reaction of aryl halides with arylboronic acid.

2. Experimental

2.1. Materials and instruments

All chemicals used were of the analytical grade or of the highest purity grade available. Gold chloride was purchased from

* Corresponding author. Tel.: +91 79 26300969; fax: +91 79 26308545; mobile: +91 9427628565.

E-mail address: hk_ss.in@yahoo.com (H. Kaur).

Aldrich. Aryl halides and aryl nitro compounds were purchased from Aldrich or Merck. Dichloromethane (DCM), diethyl ether (Et_2O), NaOH and NaBH_4 were purchased from Finar Chemicals. Amberlite XAD-4 (surface area $725 \text{ m}^2 \text{ g}^{-1}$ mesh size 20–40) was purchased from Aldrich. Water used in all experiments was purified by the Millipore-Q system. All glassware was thoroughly cleaned with freshly prepared 3:1 HCl/HNO₃ (aqua regia) prior to use.

CEM benchmate microwave reactor was used for microwave heating. UV-visible absorption spectra were acquired on a Jasco V-570 UV-visible spectrophotometer. X-ray diffraction was recorded on SEIFERT FPM, XRD 7 using Cu K α radiation ($\lambda = 1.5418$) and filter of nickel. Scanning Electron Microscopy (SEM) image of the bead was taken on a Leo 1430 VP Electron Microscope after coating it with palladium. High resolution transmission electron microscopy (HR-TEM) pictures were taken using a Hitachi (H-7500) instrument. The swollen resin beads were milled and a drop of alcoholic suspension was placed onto a 200 mesh carbon coated copper grid. It was then dried to evaporate the solvent and used for microscopy. GC-MS measurements were carried on Perkin-Elmer USA Auto system XL. ¹H NMR spectra were recorded on a Bruker Advance II 400 NMR spectrometer. Inductively coupled plasma atomic emission spectroscopy (ICP-AES) measurements were carried out on a HJY Ultima-2 instrument: power 1000 W, nebulizer flow 1.29, nebulizer pressure 2.96, wave length 242.795 nm. LOD (limit of detection) as determined by signal to noise ratio was found to be 0.25 mg/L.

2.2. Preparation of resin supported gold nanoparticles (resin-AuNPs)

The resin supported gold nanoparticles were synthesized by a method developed in our lab. Amberlite XAD-4 beads (5.0 g) were washed repeatedly with hot water to remove salts, swollen in ethanol and then equilibrated with 10 mL of 1 mmol solution of gold chloride in ethanol. After 1 h, excess solution was drained and the metal was reduced by passing cold aqueous NaBH_4 (0.1 mol dm⁻³) solution. The resin particles were further washed with water to remove excess reagent and stored in ethanol.

2.3. Reduction of nitro compound by resin-AuNPs

In a typical reduction protocol, 100 mg of catalyst was added to 20 mL of methanol/water (1:1) solution containing 0.5 mmol of nitro compound and 5 mmol of NaBH_4 . The mixture was vigorously stirred at 40 °C. The reaction was monitored by Thin Layer Chromatography (TLC) and reaction mixture was quenched by extracting the organic derivatives with ethyl acetate. The solvent was evaporated under vacuum to give crude product of corresponding amine compound. Further purification was done through column chromatography. The products were confirmed by their melting points and ¹H NMR spectroscopy.

2.4. Suzuki-Miyaura coupling catalyzed by resin-AuNPs

Into a 10 mL vial, phenylboronic acid (1.5 mmol), aryl iodide (1.0 mmol), sodium hydroxide (3.0 mmol), ethanol (2.0 mL), water (1.0 mL) and catalyst (200 mg wet resin) were taken and heated in a CEM microwave (140 °C, 300 w) for 12 min. The reaction was quenched by filtering the hot solution in 10 mL of cold water. The resulting solution was extracted with $\text{Et}_2\text{O}/\text{DCM}$ (2 × 5 mL). The combined extracts were dried over anhydrous MgSO_4 and the solvents were removed under vacuum. The crude products were then recrystallized from appropriate solvent and characterized by ¹H NMR.

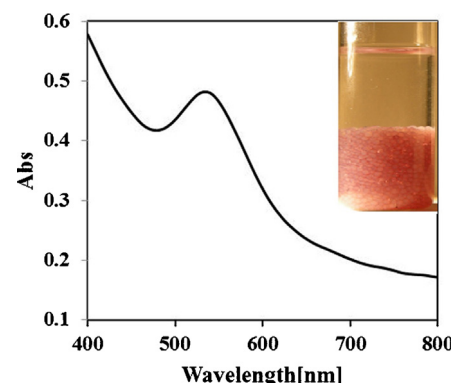


Fig. 1. UV-visible spectrum for the resin-AuNPs, inset: picture of resin-AuNPs. Beads taken with lateral illumination.

3. Results and discussion

3.1. Synthesis and characterization of resin supported AuNPs

Amberlite XAD-4 is a neutral, non-functional, hydrophobic, macroporous, commercial and cross-linked polystyrene resin. The resin is chemically and mechanically stable and there is no interference with the reaction conditions. While the presence of ligands/functional groups on a resin can control the size and stability of the nanoparticles, they have a negative influence from the catalytic activity point of view i.e. reducing the interaction of catalytic sites with the substrate. Hence, it seemed prudent to use the resin as a support for nanoparticle synthesis. The resin beads turn pink on impregnation of gold nanoparticles and since no other stabilizing agent was used it is assumed that the nanoparticles are trapped in the polymer network and stabilized solely by the steric factor/electrostatic interaction of the benzene rings.

AuNPs exhibit strong surface plasmon resonance (SPR) absorption band that is absent in the spectrum of the bulk metal. This band is dependent on the size, shape and aggregation of AuNPs. Therefore, UV-visible spectroscopy is a useful tool to estimate nanoparticle size, concentration, and aggregation level. In the present case, the resin-AuNPs beads were milled with ethanol and the solution centrifuged for 10 s. The supernatant solution was analyzed by spectrophotometer against a blank prepared from similarly treated resin beads. The SPR band maximum for AuNPs was thus observed at 535 nm which is characteristic of gold nanoparticles (Fig. 1). The red shift observed in the SPR band at 535 nm (Mie theory predicts SPR at 510–515 nm for gold particles of 3–8 nm as measured by TEM) can be due to stabilization of the nanoparticles by the π electron cloud of the benzene ring [19].

The XRD pattern of the powdered resin beads is shown in Fig. 2. The resin particles did not show any peak, only a broad hump was observed, which indicated the amorphous nature of the polymer matrix. When these beads were impregnated with gold nanoparticles, characteristic peaks of gold at $2\theta = 38.5$ and 44.2 (JCPDS No. 04-0784) were observed, corroborating the immobilization of the nanoparticles onto the resin beads. The bands were identified as (1 1 1) and (2 0 0) reflections corresponding to the fcc lattice of gold nanoparticles [20]. The broad nature of the bands was also indicative of the nanosize of the particles.

SEM image of the resin beads did not show any particles or agglomerations on the surface (Fig. 3). Thus, we inferred that all the particles are trapped inside the matrix of the resin. TEM was used to study the shape and size of nanoparticles. TEM pictures of AuNPs taken after milling the beads (Fig. 4) showed spherical nanoparticles embedded in polymer matrix. The size of the nanoparticles varies between 3 and 8 nm. To determine the amount of gold loaded

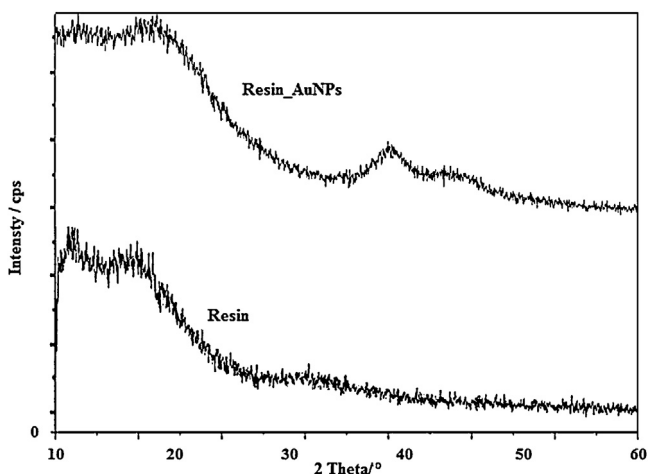


Fig. 2. XRD pattern of the resin-AuNPs.

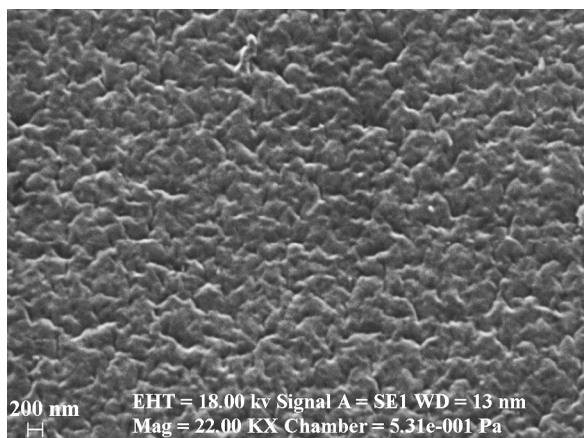


Fig. 3. SEM image of resin-AuNPs.

onto the resin, 500 mg of resin was incinerated in a crucible for 4 h at 550 °C. The residue was dissolved in 1 mL Aqua regia and diluted to 10 mL with distilled water. The average concentration of gold (3 trials) as determined by ICP-AES was found to be 0.0032 mmol/g (0.630 mg/g) of the resin.

3.2. Reduction of nitro compounds by resin-AuNPs

Reduction of nitro compounds is widely used in different industries like agrochemicals, dyes, pharmaceuticals, etc. Many reducing agents have been utilized for their reduction, the most classic being metallic reagents in the presence of an acid. However, this methodology is messy and environmentally hazardous [21] and therefore, synthetic routes involving cleaner and cheaper alternatives are necessary. One such methodology is to employ NaBH₄ in water as the hydride source in the presence of catalyst [22–24]. This reaction is also used widely to evaluate catalytic activity of gold nanoparticles. The versatility of resin-AuNPs catalyst in reducing different nitro derivatives is presented in Table 1. The striking feature of our catalyst is the quantitative reduction of halo nitro benzenes and nitro amines (Table 1). In case of 4-nitrobenzaldehyde (entry 6) we found selective reduction of aldehyde over nitro group and the major product was 4-nitrobenzyl alcohol. However, on increasing the amount of sodium borohydride 4-aminobenzyl alcohol was obtained as the sole product. In the presence of olefinic bond (entry 7) surprisingly the double bond was reduced in preference to the nitro group and major product was 2-nitrophenyl ethane and not the expected phenyl ethenamine. Again on increasing the concentration of sodium borohydride and time we could isolate 2-phenylethylamine in quantitative yield. The method can be used as a one step process for the synthesis of phenylethylamines.

The kinetics of the catalytic reduction reaction was studied in a standard quartz cuvette with 1 cm path length and 4.5 mL volume. 2.27 mL of water was mixed with 30 μL (10⁻² M) 4-nitrophenol solution, and finally 200 μL freshly prepared NaBH₄ solution (10⁻¹ M) was added. After mixing these solutions, 5 mg of AuNPs were added in cuvette to study the reduction reaction. UV-visible spectra were recorded at every 10 min interval in the range of 200–500 nm for at least 60 min at 25 and 35 °C. The rate constant was determined by measuring the change in absorbance (Fig. 5) of a peak at 400 nm, the initially observed peak for the nitrophenolate ion, as a function of time. The peak shows a gradual decrease in intensity with time and a new peak appeared at 295 nm indicating the formation of 2-aminophenol. The reaction shows a pseudo-first-order kinetics with respect to 4-nitrophenol and the rate constants were calculated to be 1.7 × 10⁻² s⁻¹ and 2.55 × 10⁻² s⁻¹ at 25 °C and 35 °C respectively. The reduction was found to occur only in the presence of our nanocatalyst and no reduction occurred in the absence of AuNPs. Thus, indicating that the catalytic reduction occurs at the surface of nanocatalyst. It was also observed from Fig. 6 that the rate of the reaction increased with the increase in the temperature. Table 2 shows a comparison of the rate constants for the present method with those reported in the

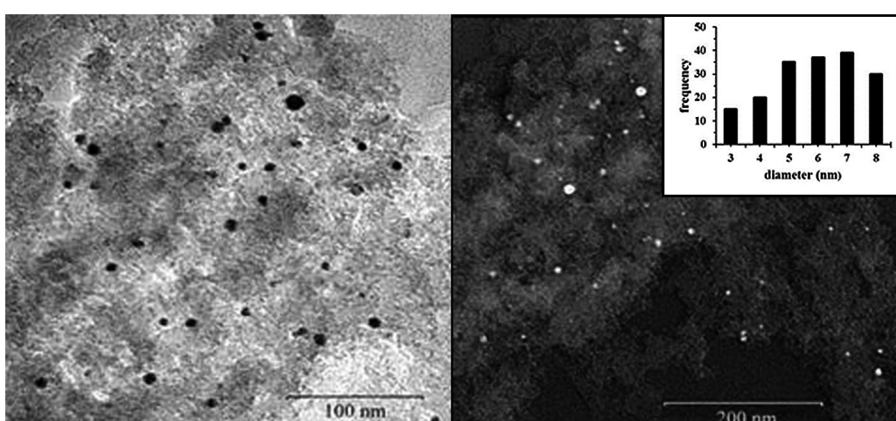


Fig. 4. TEM image of resin-AuNPs at 100 and 200 nm resolution.

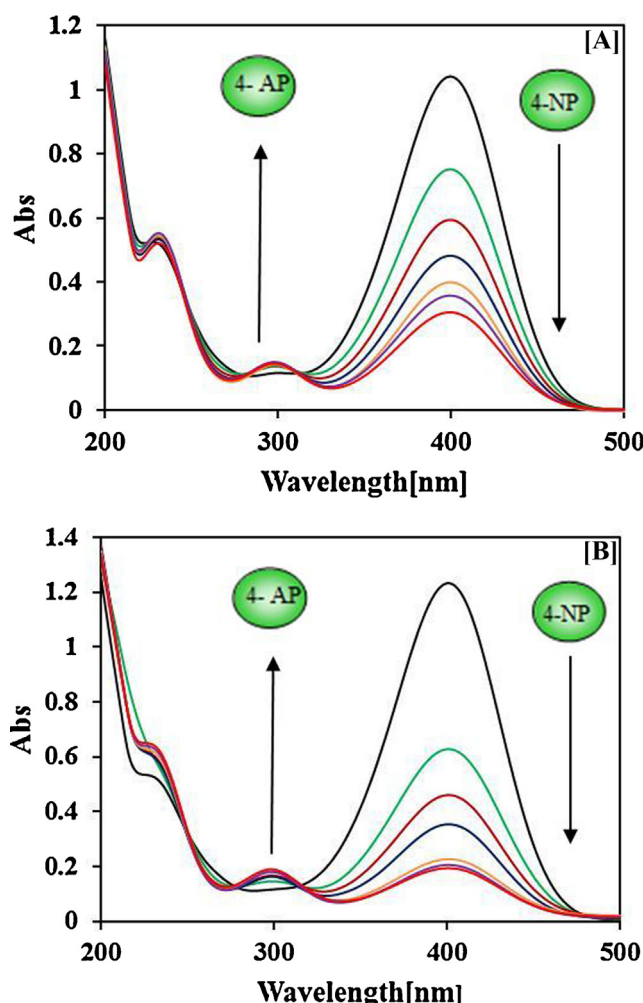


Fig. 5. UV-visible spectra for the reduction of 4-nitrophenol measured at 10 min intervals (a) at 25 °C (b) at 35 °C.

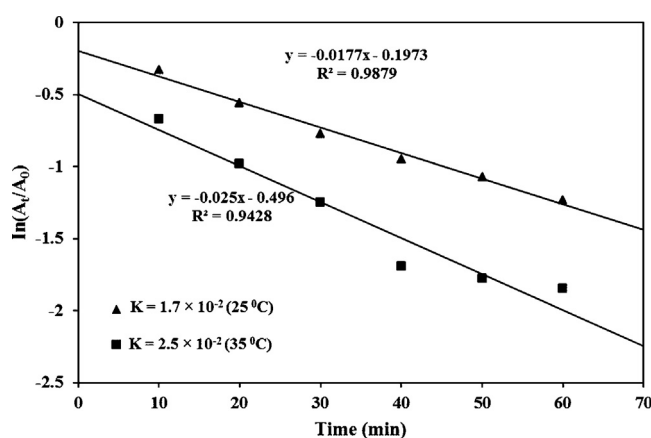


Fig. 6. Plot of $\ln(A_t/A_0)$ versus time for the reduction of 4-nitrophenol.

Table 2

Systematic literature survey of rate constant at room temperature for the reduction of 4-nitrophenol.

Entry	Sample	Carrier system	$k (s^{-1})$	Ref.
1	Resin-AuNPs	Non-ionic resin	2.5×10^{-2}	This work
2	AuNPs	PAMAM dendrimer	$1.78\text{--}13.2 \times 10^{-3}$	[25]
3	Au-resin	Ion-exchange resin	0.16×10^{-3}	[26]
4	AgNPs/GR-G3.0 PAMAM	PAMAM dendrimer	21.7×10^{-3}	[27]
5	Au/PMMA	Poly(methyl methacrylate)	7.9×10^{-3}	[28]
6	PEI capped AuNPs	Polyelectrolyte	5.2×10^{-2}	[29]

Table 1
Resin-AuNPs catalyzed reduction of aromatic nitroarenes.

Entry	Substrate	Product	Time (min) at 40 °C	^a Yield (%)
1	<chem>O=[N+]([O-])c1ccccc1</chem>	<chem>Nc1ccccc1</chem>	20	85
2	<chem>O=[N+]([O-])c1cc(O)ccc1</chem>	<chem>Nc1cc(O)ccc1</chem>	20	82 (85) ^b
3	<chem>O=[N+]([O-])c1ccc(N)cc1</chem>	<chem>Nc1ccc(N)cc1</chem>	25	95
4	<chem>O=[N+]([O-])c1ccc(N)c2ccccc21</chem>	<chem>Nc1ccc(N)c2ccccc21</chem>	25	90
5	<chem>O=[N+]([O-])c1ccc(Br)cc1</chem>	<chem>Nc1ccc(Br)cc1</chem>	25	90
6	<chem>O=[N+]([O-])c1ccc(C=O)cc1</chem>	<chem>Nc1ccc(CO)cc1</chem>	25	85
7	<chem>O=[N+]([O-])c1ccccc1</chem>	<chem>[H]C(=O)[N+]([O-])c1ccccc1</chem>	30	80
		<chem>[H]2C([H])[N+]([O-])c1ccccc1</chem>		

Aromatic nitroarenes (0.5 mmol); NaBH₄ (5 mmol); Au catalyst (100 mg resin); 20 mL of MeOH/H₂O (1:1); 40 °C 20 min.

^a Isolated yield.

^b % Conversion.

literature. The activation energy of the reaction at different temperatures was calculated from the Arrhenius equation. The activation energy calculated for the p-nitrophenol (4-NP) to p-aminophenol (4-AP) test reaction is 29.8 ± 2 kJ per mole. The apparent activation energies for the same reaction carried out with different gold nanoparticles (various shapes, different supports) range from 30 to 58 kJ per mole.

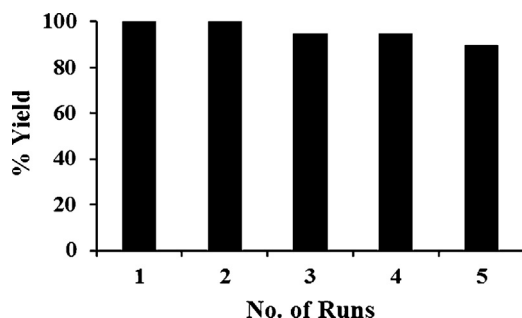


Fig. 7. Recycling of the catalyst for the reduction of 4-nitrophenol.

Recyclability of the resin-AuNPs catalyst was also investigated. The resin beads were recovered by simple filtration and were washed with hot water/ethanol to remove any sorbed products. The resin-AuNPs were reused without obvious loss of their catalytic activity, up to four cycles. Recyclability of the resin is shown in Fig. 7.

3.3. Suzuki-Miyaura reaction catalyzed by resin-AuNPs

Suzuki reaction of aryl halides with phenylboronic acid, which is predominately catalyzed by palladium (Pd) catalysts, is a powerful and convenient synthetic method for the generation of biaryl in organic chemistry. There are only a few reports of AuNPs catalyzed Suzuki reaction. Han et al. [30] first reported the activity of PATP polymer-stabilized gold nanoparticles for Suzuki-Miyaura cross-coupling reaction of aryl halides with arylboronic acids in water. Li et al. [31] reported AuNPs supported on graphene as active catalyst for the Suzuki reaction of aryl halides with arylboronic acid in water under aerobic conditions. We explored the catalytic activity of resin-AuNPs for the Suzuki reaction. The reaction was successfully carried out in methanol/water under aerobic conditions in a microwave. It was also observed that water was required for the reaction as no reaction took place when pure ethanol was used.

The effect of various parameters such as time, catalyst concentration and effect of base were studied taking the coupling of 4-iodoanisole and phenylboronic acid as the standard reaction. The time course of the reaction was studied by quenching the reaction at different time intervals and the reaction mixture was analyzed by GC-MS. It was observed that after 12 min (Fig. 8) the peak for 4-iodoanisole disappeared completely and 4-methoxybiphenyl was identified as the sole coupling product by its mass spectrum. The effect of base on the reaction was also studied and it was observed that three moles of NaOH were required for the completion of the

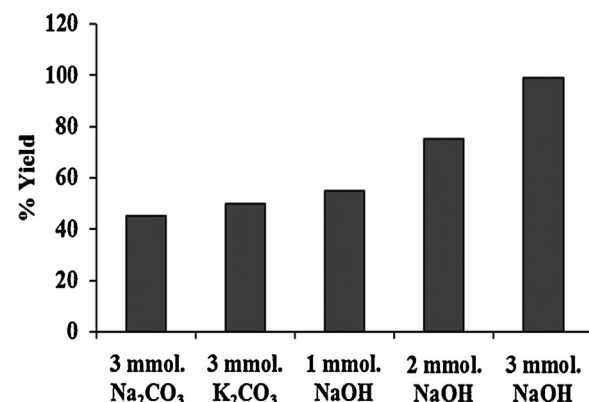


Fig. 9. Effect of base on the yield of standard Suzuki-Miyaura coupling reaction.

reaction. The reaction did not proceed to completion when either Na_2CO_3 or K_2CO_3 were used as base (Fig. 9).

The effect of catalyst concentration was carried out by varying the amount of catalyst while keeping the other parameters constant. It was observed that 200 mg of resin was sufficient to complete the reaction (Fig. 10). The TON and TOF (h^{-1}) were calculated to be 1666 and 8330, respectively.

We also carried out Suzuki cross-coupling with other substituted iodobenzenes containing both electron withdrawing and electron releasing groups. The results are summarized in Table 3. In all the cases very high conversion of iodobenzenes was observed in short reaction times. Bromobenzene and chlorobenzene were also used for coupling with phenylboronic acid (Table 3, entries 8 and 9). Their reactivities were however, found to be lower than that of iodobenzene. This decrease may be attributed to the differences in the strengths of C—I bond, C—Br bond and C—Cl bond. The recyclability of the catalyst was also investigated and the results are shown in Fig. 11. The catalysts was recovered by simple filtration and washed with alcohol/water and reused. The slight yield loss was observed after five cycles.

3.4. Leaching studies of the catalyst

Leaching can decrease the efficiency and service life of a catalyst. In order to study the leaching of catalyst during the reaction, hot filtration test was performed in both the reactions. In case of nitro group reduction the resin beads were filtered off from the reaction mixture after 5 min and the filtrate was monitored for continued activity by UV-visible spectroscopy. The results revealed that after the removal of the resin particles, the reaction stopped (Fig. 12), indicating the absence of active gold species in the reaction mixture.

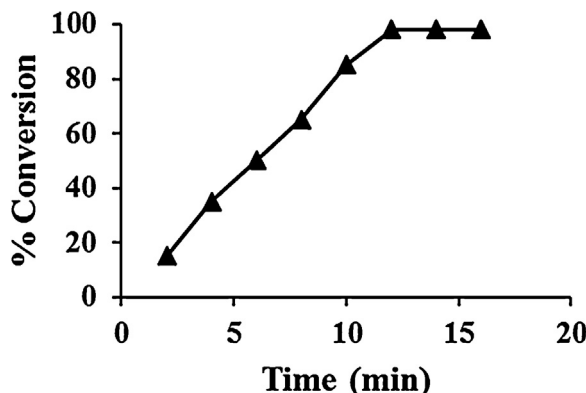


Fig. 8. Time course of Suzuki-Miyaura reaction between phenylboronic acid and 4-iodoanisole.

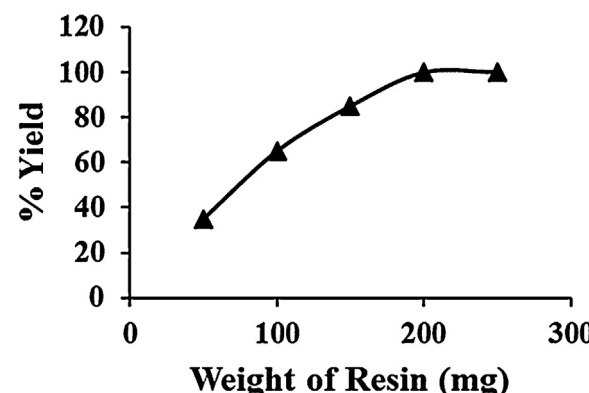


Fig. 10. Effect of catalyst concentration on the standard Suzuki-Miyaura coupling reaction.

Table 3
Resin-AuNPs catalyzed Suzuki-Miyaura coupling.

Entry	Aryl halide	Product	Time (min)	^a Yield (%)
1			12	80
2			12	85
3			12	85
4			12	75
5			12	80
6			15	80
7			12	75
8			20	45
9			20	Trace

Aryl halide (1.0 mmol); phenylboronic acid (1.5 mmol); Au catalyst (200 mg resin); NaOH (3.0 mmol); EtOH (2 mL); H₂O (1 mL), (microwave conditions, 140 °C, 12 min).

^a Isolated yield.

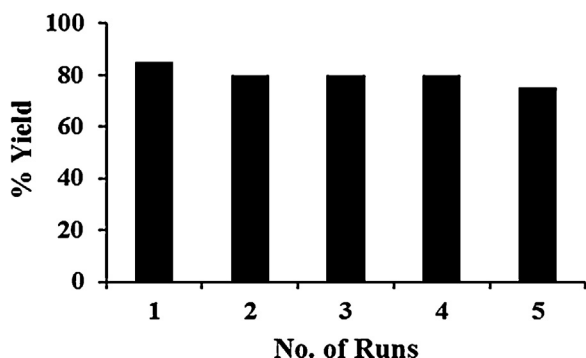


Fig. 11. Recycling of the catalyst for the standard Suzuki Miyaura coupling reaction.

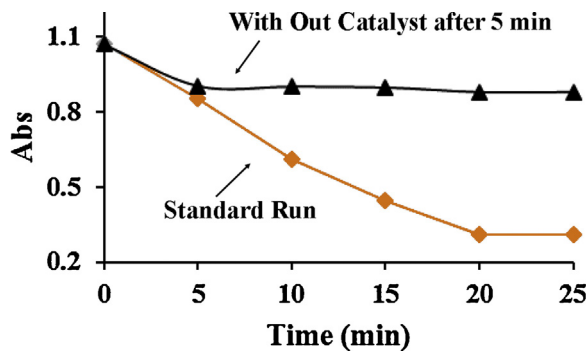


Fig. 12. Time course of the reduction of 4-nitro phenol Standard run and after filtration of resin.

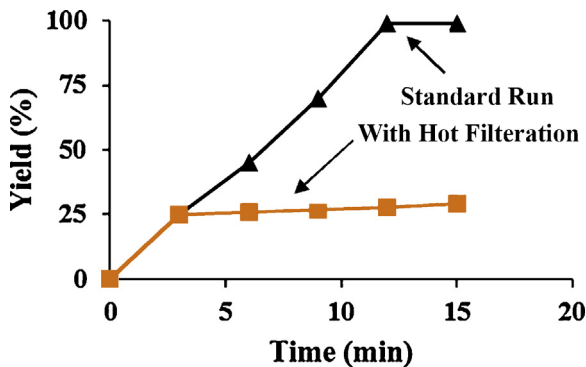


Fig. 13. Time course of the Suzuki-Miyaura reaction between phenylboronic acid and 4-Iodoanisol (standard run) and after hot filtration of the resin.

Additionally the reaction mixture was evaporated and the residue was analyzed for the presence of gold by ICP-AES. The absence of gold in the reaction mixture indicated that no leaching of gold has taken place.

In case of Suzuki reaction the resin was removed from the hot reaction mixture by filtration after 3 min and the filtrate was monitored for continued activity. The results indicate (Fig. 13) that the reaction did not proceed after the removal of the catalyst. Additionally in the standard reaction mixture, the solvent was evaporated and the residue was analyzed for the presence of gold by ICP-AES. Au could not be estimated in the solution. The absence of leaching as indicated by the hot filtration test and the reduction of olefinic bond points toward the heterogeneous nature of catalysis.

4. Conclusion

In summary, we report that Amberlite XAD-4 can be used to synthesize highly stable supported AuNPs. The catalytic activity of the

AuNPs was studied for the reduction of nitro group and the Suzuki-Miyaura cross coupling reaction. The rate constant and the apparent activation energy calculated for the reduction of 4-nitrophenol is comparable to the best reported in the literature. The catalyst can also be used for one step synthesis of phenylethylamines. The catalyst can be utilized for Suzuki-Miyaura cross coupling reaction of various aryl halides. However, the activity is less compared to similarly prepared palladium nanoparticles [16]. It is also noteworthy that the catalyst showed excellent recyclability for both the reactions.

Acknowledgements

Authors are grateful to the UGC, New Delhi for the BSR fellowship. SAIF, Panjab University, Chandigarh, for the NMR spectra, Sicart, Vallabh Vidhya Nagar, Gujarat, for GC-MS and TEM. CSM-CRI, Bhavnagar, for SEM pictures. Dr. Sareen PRL, Ahmedabad for ICP-AES studies, O₂H Ahmedabad for ESI Mass.

Appendix A. Supplementary data

Supplementary material related to this article can be found, in the online version, at <http://dx.doi.org/10.1016/j.molcata.2013.10.004>.

References

- [1] G. Schmid, in: K.J. Blabunde (Ed.), *Nanoscale Materials in Chemistry*, Wiley-VCH, New York, 2001.
- [2] A. Corma, H. Garcia, *Chem. Soc. Rev.* 37 (2008) 2096–2126.
- [3] M.N. Zhang, L. Su, L.Q. Mao, *Carbon* 44 (2006) 27–36.
- [4] J.H. Kim, H.H. An, H.S. Kim, Y.H. Kim, C.S. Yoon, *J. Colloid Interface Sci.* 337 (2009) 289–293.
- [5] M. Valden, X. Lai, D.W. Goodman, *Science* 281 (1998) 1647–1650.
- [6] K. Qian, S.S. Lv, X.Y. Xiao, H.X. Sun, J.Q. Lu, M.F. Luo, W.X. Huang, *J. Mol. Catal. A: Chem.* 306 (2009) 40–47.
- [7] D. Andreeva, V. Idakiev, T. Tabakova, L. Ilieva, *Catal. Today* 72 (2002) 51–57.
- [8] S.Y. Lee, M. Yamada, M. Miyake, *Carbon* 43 (2005) 2654–2663.
- [9] T. Noguchi, K. Matsui, N.M. Islam, Y. Hakuta, H. Hayashi, *J. Supercrit. Fluids* 46 (2008) 129–136.
- [10] L. Wen, J.K. Fu, P.Y. Gu, B.X. Yao, Z.H. Lin, J.Z. Zhou, *Appl. Catal. B* 79 (2008) 402–409.
- [11] D.H. Wang, Z.P. Hao, D.Y. Cheng, X.C. Shi, C. Hu, *J. Mol. Catal. A: Chem.* 200 (2003) 229–238.
- [12] M. Boronat, A. Corma, F. Illas, J. Radilla, T. Rodenas, M.J. Sabater, *J. Catal.* 278 (2011) 50–58.
- [13] H. Yang, K. Nagai, T. Abe, H. Homma, T. Norimatsu, R. Ramaraj, *Appl. Mater. Interface* 1 (2009) 1860–1864.
- [14] H.F. Li, Z.L. Zheng, M.N. Cao, R. Cao, *Micropor. Mesopor. Mater.* 136 (2010) 42–49.
- [15] K. Ohno, K.M. Hoh, Y. Tsuji, T. Fubuda, *Macromolecules* 35 (2002) 8989–8993.
- [16] H. Miyamura, R. Matsubara, Y. Miyazaki, S. Kobayashi, *Angew. Chem. Int. Ed.* 46 (2007) 4151–4154.
- [17] H. Kaur, D. Shah, U. Pal, *Catal. Commun.* 12 (2011) 1384–1388.
- [18] D. Shah, H. Kaur, *J. Mol. Catal. A: Chem.* 359 (2012) 69–73.
- [19] M. Daniel, D. Astruc, *Chem. Rev.* 104 (2004) 293–346.
- [20] S. Panigrahi, S. Basu, S. Praharaj, S. Pande, S. Jana, A. Pal, S.K. Ghosh, *J. Phys. Chem. C* 11 (2007) 4596–4605.
- [21] M.L. Crossley, *Ind. Eng. Chem.* 14 (1922) 802–805.
- [22] Y. Mei, G. Sharma, Y. Lu, M. Ballauff, *Langmuir* 21 (2005) 12229–12234.
- [23] M. David, D.S. Bhattacharjee, Y. Wen, L.M. Bruening, *Langmuir* 25 (2009) 1865–1871.
- [24] D. Astruc, F. Lu, J. Ruiz Aranzaes, *Angew. Chem. Int. Ed.* 44 (2005) 7852–7872.
- [25] K. Hayakawa, T. Yoshimura, K. Esumi, *Langmuir* 19 (2003) 5517–5521.
- [26] S. Praharaj, S. Nath, S. Ghosh, S. Kundu, T. Pal, *Langmuir* 20 (2004) 9889–9892.
- [27] R. Rajesh, R. Venkatesan, *J. Mol. Catal. A: Chem.* 359 (2012) 88–96.
- [28] K. Kuroda, T. Ishida, M. Haruta, *J. Mol. Catal. A: Chem.* 298 (2009) 7–11.
- [29] P. Veerakumara, M. Velayudham, K. Lub, S. Rajagopala, *Appl. Catal. A: Gen.* 439/440 (2012) 197–205.
- [30] J. Han, Y. Liu, R. Guo, *J. Am. Chem. Soc.* 131 (2009) 2060–2061.
- [31] Y. Li, X. Fan, J. Qi, J. Ji, S. Wang, G. Zhang, F. Zhang, *Mater. Res. Bull.* 45 (2010) 1413–1418.